Integrating NGS-derived mutational profiling in the diagnosis of multiple lung adenocarcinomas

Ezer, Nicole; Wang, Hangjun; Corredor, Andrea Gomez; Fiset, Pierre Olivier; Baig, Ayesha; van Kempen, Léon C; Chong, George; Issac, Marianne S M; Fraser, Richard; Spatz, Alan

Published in:
Cancer Treatment and Research Communications

DOI:
10.1016/j.ctarc.2021.100484

Publication date:
2021

Cancer Treatment and Research Communications 29 (2021) 100484

Contents lists available at ScienceDirect

Cancer Treatment and Research Communications

journal homepage: www.sciencedirect.com/journal/cancer-treatment-and-research-communications

Integrating NGS-derived mutational profiling in the diagnosis of multiple lung adenocarcinomas

Nicole Ezer [a,b], Hangjun Wang [c,d,e], Andrea Gomez Corredor [d,f], Pierre Olivier Fiset [c,d], Ayesha Baig [c,d], Léon C. van Kempen [d,f,g], George Chong [d,f], Marianne S.M. Issac [h,i], Richard Fraser [c,d], Alan Spatz [c,d,e], Jean-Baptiste Riviere [d,f], Philippe Broët [j,k], Jonathan Spicer [l], Sophie Camilleri-Broët, MD, PhD [c,d,*]

[a] Department of Medicine, Division of Respirology, McGill University Health Center, 1001 Decarie Blvd., Montreal, QC, Canada
[b] Centre for Outcomes Research and Evaluation - Research Institute of the McGill University Health Center, Montreal, 1001 Decarie Blvd., QC, Canada
[c] Division of Pathology, McGill University Health Center, 1001 Decarie Blvd., Montreal, QC, Canada
[d] OPTILAB-MUHC & Department of Laboratory Medicine, 1001 Decarie Blvd., Montreal, QC, Canada
[e] Research Molecular Pathology Center, Lady Davis Institute, 3755 Côte Ste-Catherine Road, Montreal, QC, Canada
[f] Division of Molecular Genetics, McGill University Health Center, 1001 Decarie Blvd., Montreal, QC, Canada
[g] University Medical Center of Groningen, PO box 30.001, 9700 RB, Groningen, Netherlands
[h] Research Institute of the McGill University Health Centre, 1001 Decarie Blvd, Montreal, QC, Canada
[i] Department of Clinical and Chemical Pathology, Faculty of Medicine, Cairo University, El Saray St., El Manial, Postal Code 11956, Cairo, Egypt
[j] UMR 1018, INSERM, CESP, Paris-Saclay University, Faculty of Medicine, Paul-Brousse Hospital AP-AP, Villejuif, France
[k] Research Center, CHU Ste-Justine, University of Montreal, 3175 Côte-Sainte-Catherine Road, H3T 1C5, Montreal, QC, Canada
[l] Division of Thoracic and Upper GI Surgery, McGill University Health Center, 1650 Cedar Avenue Montreal, H3G 1A4, Montreal, QC, Canada

ARTICLE INFO

Keywords:
Multiple primary lung cancers
Intrapulmonary metastases
NGS
Comprehensive histologic assessment
Probabilistic model

ABSTRACT

MicroAbstract: Integration of Next Generation Sequencing (NGS) information for use in distinguishing between Multiple Primary Lung Cancer and intrapulmonary metastasis was evaluated. We used a probabilistic model, comprehensive histologic assessment and NGS to classify patients. Integrating NGS data confirmed initial diagnosis ($n = 41$), revised the diagnosis ($n = 12$), while resulted in non-informative data ($n = 8$). Accuracy of diagnosis can be significantly improved with integration of NGS data.

Background: Distinguishing between multiple primary lung cancers (MPLC) and intrapulmonary metastases (IPM) is challenging. The goal of this study was to evaluate how Next Generation Sequencing (NGS) information may be integrated in the diagnostic strategy.

Patients and Methods: Patients with multiple lung adenocarcinomas were classified using both the comprehensive histologic assessment and NGS. We computed the joint probability of each pair having independent mutations by chance (thus being classified as MPLC). These probabilities were computed using the marginal mutation rates of each mutation, and the known negative dependencies between driver genes and different gene loci. With these NGS-driven data, cases were re-classified as MPLC or IPM.

Results: We analyzed 61 patients with a total of 131 tumors. The most frequent mutation was *KRAS* (57.3%) which occured at a rate higher than expected ($p < 0.001$) in lung cancer. No mutation was detected in 25/131 tumors (19.1%). Discordant molecular findings between tumor sites were found in 46 patients (75.4%); 11 patients (18.0%) had concordant molecular findings, and 4 patients (6.6%) had concordant molecular findings at 2 of the 3 sites. After integration of the NGS data, the initial diagnosis was confirmed for 41 patients (67.2%), the diagnosis was revised for 12 patients (19.7%) or was considered as non-informative for 8 patients (13.1%).

Conclusion: Integrating the information of NGS data may significantly improve accuracy of diagnosis and staging.

* Corresponding author at: Division of Pathology, McGill University Health Center, 1001 Decarie Blvd., Montreal, Quebec, H4A 3J1 Canada.
E-mail address: sophie.camilleri-broet@mcgill.ca (S. Camilleri-Broët).

https://doi.org/10.1016/j.ctarc.2021.100484

Available online 29 October 2021

Introduction

With improvements in high-resolution imaging and the advent of low dose CT screening programs, the incidence of early stage non-small cell lung cancer (NSCLC) and multiple primary lung cancers (MPLC) has grown. The TNM 8th edition for lung cancer [1]' [2]' [3]' [4]' [5] established criteria to help classifying multiple lung tumours in four categories: separate tumor nodules (i.e. intra-pulmonary metastases, IPM); multiple primary lung cancers (synchronous or metachronous, MPLC); multifocal ground glass/lepidic tumours (corresponding histologically to atypical adenomatous hyperplasia, adenocarcinoma in situ, minimally invasive adenocarcinoma and lepidic predominant invasive adenocarcinoma); and pneumonic-type lung cancers (typically invasive mucinous adenocarcinoma). While multifocal ground glass/lepidic tumours and pneumonic-type lung cancers have somewhat different clinical presentations, reliably differentiating pathologically between two (or more) adenocarcinomas as either MPLC or IPM remains an important challenge for clinicians and pathologists.

In their seminal study of multiple primary lung cancers, Martini and Melamed [6] were the first to define a list of criteria to distinguish between second primary and intra-pulmonary metastases. These criteria were based on tumor morphology, presence or absence of carcinoma in situ, presence or absence of vascular invasion and/or distant metastases. Given the subjectivity of these criteria, the comprehensive histologic assessment (CHA) was introduced to improve the attribution of a MPLC or IPM. The CHA identifies the main architectural pattern, the percentage of minor histological patterns (e.g. solid, lepidic, papillary, acinar) in each tumor, as well as cytological characteristics[7].

However, applying the CHA is challenging when tumors display significant intra-tumoral heterogeneity of architectural and cytological patterns. Furthermore, the value of a shared main tumor architecture may be low when dealing with highly common architectures, such as an acinar pattern which is seen in more than 50% of adenocarcinomas. In such cases, it is highly likely that the main acinar architecture is concordant by chance rather than being a result of shared clonal origin resulting from a metastatic process. Additionaly, the rate of inter-observer disagreement of cytological and architectural patterns is still not negligible, even between expert lung pathologists[8]. Finally, in non-surgical biopsies, histological classification cannot be used in small specimens arising from core lung biopsies or cytology specimens.

The CHA shows only fair correlation with genomic-based studies[9]. Next-generation sequencing testing (NGS), routinely performed in advanced stage lung cancer for targeted therapy, is not widely used for early stage lung cancer and to differentiate between MPLC and IPM. Published retrospective case series have shown promise with regards to distinguishing MPLC and IPM, [10–12] but its impact on reclassification when integrated prospectively into routine clinical practice has not been quantified. In our study we aim to evaluate the clinical impact of routine NGS use for patients with multiple adenocarcinomas.

Patients and methods

Patients with multiple ($\geq$ 2) invasive non-small cell lung cancers (non-squamous non-neuroendocrine), either synchronous or metachronous were identified prospectively from July 2016 to February 2020 at the McGill University Health Center (MUHC) pathology database.

Patients with one invasive tumor and a second or more tumors with non-invasive features (e.g. adenocarcinoma in situ or microinvasive adenocarcinoma) were excluded from the study. All tumors were assessed histologically using the WHO classification, [13] and classified histologically according to the CHA. [7] Pathological staging was performed accordingly using either the AJCC 7th edition [14] (until December 2017) or the 8th edition [15] (since January 2018). The mediastinum was staged with PET scan. Endobronchial ultrasound guided lymph node biopsy was performed where clinically indicated. Cases with N1, N2 or N3 nodes identified pre-operatively were excluded.

For each patient the number of tumors, location/laterality, pathological size, histological subtype and percentage of different histological patterns for adenocarcinomas, lympho-vascular invasion, spread through air spaces (STAS), pleural invasion, lymph node stations involved, and final pTNM stage, IPM/MPLC classification on histology was collected. PD-L1 immunohistochemistry was performed using the Dako PD-L1 22C3 (PharmDx, Agilent, Santa Clara, CA, USA), with specimens considered adequate when a total of 100 or more viable tumor cells were present. Tumor cell proportion score was reported as $\geq$ 50% versus $<$ 50%. ALK translocation detection was carried out using an immunohistochemistry screening, using the D5F3 clone XP® Rabbit mAb #3633 (Cell Signaling Technology, Whitby, ON, Canada) and the EnVision™ FLEX, High pH DaB detection kit from Agilent-Dako, Agilent, Santa Clara, CA, USA.

Up until November 2018, the NGS analysis was done using the Illumina TruSight Tumor 15 (TST15 panel, Illumina, San Diego, CA, USA) on a MiSeq platform (Illumina, San Diego, CA, USA). The panel included the following genes: *AKT1, BRAF, EGFR, ERBB2, FOXL2, GNA11, GNAQ, KIT, KRAS, MET, NRAS, PDGFRA, PIK3CA, RET, TP53*. Since December 2019, the Ampliseq Focus Panel (52 genes) for Illumina was used on a MiSeq. This includes single- nucleotide DNA variants (SNVs) and small insertions/deletions (indels) in 35 genes (*AKT1, ALK, AR, BRAF, CDK4, CTNNB1, DDR2, EGFR, ERBB2, ERBB3, ERBB4, ESR1, FGFR2, FGFR3, GNA11, GNAQ, HRAS, IDH1, IDH2, JAK1, JAK2, JAK3, KIT, KRAS, MAP2K1, MAP2K2, MET, MTOR, NRAS, PDGFRA, PIK3CA, RAF1, RET, ROS1, and SMO*), copy-number variants (CNVs) in 19 genes (*ALK, AR, BRAF, CCND1, CDK4, CDK6, EGFR, ERBB2, FGFR1, FGFR2, FGFR3, FGFR4, KIT, KRAS, MET, MYC, MYCN, PDGFRA, and PIK3CA*), and recurrent gene fusions and other aberrant splicing events involving 23 driver genes (*ABL1, ALK, AKT3, AXL, BRAF, EGFR, ERBB2, ERG, ETV1, ETV4, ETV5, FGFR1, FGFR2, FGFR3, MET, NTRK1, NTRK2, NTRK3, PDGFRA, PPARG, RAF1, RET, ROS1*). Variants have been routinely interpreted and categorized based on their clinical impact, as per standards and guidelines in the field [16].

Interpretation of the results and assignation into subtypes

The main aim of this study was to analyze the potential added value of reflex NGS testing in the classification of IPM and MPLC.

Initial classification to the MPLC or IPM stage was routinely performed histologically by the initial pathologist using the CHA[7]. NGS was performed on each tumor and the results were compared. Prospectively, three molecular categories were present: (i) tumors with discordant molecular results (different gene mutations) (ii) tumors with concordant molecular results (identical highly common mutations found in lung cancer or no mutations), (iii) tumors with concordant results with mutations having a low frequency. In the first category, the molecular analysis favours MPLC. The second category involved tumors having either no mutation or the highly frequent *KRAS* mutation *KRAS* G12C (c.34G $>$ *T*; p. Gly12Cys). In the later case, we considered the molecular analysis as "non-contributory" and kept the initial histological diagnosis. In the third category, the IPM diagnosis was favoured. When the molecular result was discordant with the initial assignation, the treating physician was notified and/or the case was discussed in the weekly thoracic tumor board and the pathological report was amended, with a revised TNM status (Supplementary Figure 1).

Statistical analysis

The relationship between the type of multiple carcinoma (MPLC versus IPM) and clinico-pathological categorical variables were tested using the $\chi 2$ test or Fisher's exact test when appropriate. P-value $<$ 0.05 was considered as significant.

We identified estimated marginal mutation rates from the rates from The Cancer Genome Atlas (TCGA) [17] for each genetic mutation. When estimated marginal mutation rates were inferior to 1% we considered

Table 1
Clinical characteristics of 51 patients with more than one tumor foci.

	Total	IPM	MPLC	p-value
Patient's characteristics	***N* = 61**			
		***N* = 9**	***N* = 52**	
Age (median, range)	69 (48–85)	68.7(53–84)	69 (48–85)	NS
Male, N%	19(31.1%)	5(55.6%)	14(26.9%)	0.09
Female, N%	42(68.9%)	4(44.4%)	38(73.1%)	
Smoking status				
Current Smoker	21(34.4%)	2 (22.2%)	19(36.5%)	NS
Ex-smoker	29 (47.5%)	5 (55.6%)	24 (46.2%)	
Non smoker	3(4.9%)	1 (11.1%)	2 (3.8%)	
Unknown	8(13.1%)	1 (11.1%)	7 (13.5%)	
Location				
Same lobe	39(63.9%)	7(77.8%)	32(61.5%)	NS
Different lobes, ipsilateral	18(29.5%)	1(11.1%)	17(32.7%)	
Contralateral	4(6.6%)	1(11.1%)	3 (7 5.8%)	
Total number of tumor loci*				
2	41(67.2%)	6 (66.7%)	35(67.3%)	NS
3	7(11.5%)	1 (11.1%)	6(11.5%)	
>4	13(21.3%)	2 (22.2%)	11(21.2%)	
Pathological characteristics	***N* = 131**			
		***N* = 19**	***N* = 112**	
Size of tumors in cm (mean)	2.2	2.78	2.15	NS
Histological grade	***N* = 119**			
		***N* = 19**	***N* = 100**	
G1	48(40.3%)	3(15.8%)	45(45%)	
G2	35(29.4%)	3 (15.8%)	32(32%)	<0.001
G3	36(30.3%)	13 (68.4%)	23(23%)	
Main histological pattern**	***N* = 119**			
		***N* = 19**	***N* = 100**	
Lepidic	23(19.3%)	1(5.3%)	22(22%)	
Acinar	67(56.3%)	6(31.6%)	61(61%)	NS
Papillary	11(9.2%)	1 (5.3%)	10(10%)	
Micropapillary	2 (1.7%)	2 (10.5%)	0 (0%)	
Solid	16(13.4%)	9 (47.3%)	7(7%)	
	31(27%)	9/12(75%)	22/103(21.4%)	
Lymphovascular invasion (*N* = 115)				<0.001
Visceral pleura invasion (*N* = 121)	25(20.7%)	6/16 (37.5%)	19/105(18.1%)	0.07
ALK (*N* = 99)	0	0	0	NS
PD-L1: TPS≥50% (*N* = 113)	36(31.9%)	8/19(42.1%)	28/94(29.8%)	NS

MPLC: Multiple Primary Lung Cancers; IPM: Intrapulmonary Metastases; *Including invasive and non-invasive lesions (microinvasive adenocarcinomas and in situ adenocarcinomas).
**The main pathological patterns are reported for resection specimen only.

them to be equivalent to 1% to simplify the mathematical model; this would provide a more conservative estimates.

We computed for each pair, the probability of observing such pattern under the null hypothesis of the two tumors being MPLC (both mutations occurring independently from each other). If all the loci were independent, we could compute the likelihood of each pair samples by the product of the probabilities of each of the individual concordant events. However, there exist some dependencies between the so-called driver mutations. Certain pairs of mutations in driver genes are mutually exclusive (negative dependencies). We included these inter-dependencies (Supplementary Figure 2) in the probabilistic model (model defined mathematically in supplementary appendix Eq. (A.1). This allowed us, by combining these marginal mutation rates and their inter dependencies, to determine for each tumor pair a probability of observing this pair of mutations by chance alone. We considered the cases to be IPM when the probability of observing our results by chance was significantly lower than 1%, thus rejecting the null hypothesis of MPLC assignation.

Overall survival (OS) was calculated from the date of surgery or biopsy to death or last follow-up examination. Kaplan-Meier analysis was used to generate overall survival curves. Univariate Log-rank analysis was carried out to assess the prognostic influence of classification into MPLC or IPM subgroups.

Approval for the study was obtained from our institutional Research Ethics Board.

Results

Clinicopathological characteristics of the cases

A total of 61 patients with two or more invasive non-small cell non-squamous carcinomas were tested by NGS: 52 patients with two invasive adenocarcinomas and 9 patients with three invasive adenocarcinomas loci. The mean age was 69 years with a predominance of female patients (68.9%). Most patients had a smoking history (81.9%) and underwent surgical resection (16.4% lobectomy and sublobar resection, 55.7% lobectomy and 6.6% sublobar resections). For four patients, at least one tumor was diagnosed by biopsy or a cytological specimen. The tumor sites were in the same lobe in 63.9%, in ipsilateral separate lobes in 29.5% and more rarely in contralateral lobes (6.6%). One third of the patients (32.8%) had more than two tumors. As regards the pN stage, the data were available for 55 cases; 37 cases were pN0, 10 cases were pN1 and 8 cases were staged pN2.

As expected, the most common main architectural pattern was acinar (56.3%), followed by lepidic and solid (19.3% and 13.4%, respectively). Visceral pleural invasion and lymphovascular invasion (LVI) were detected in 20.7% and 27% of the cases, respectively. None of the tested tumors showed an alteration for *ALK* and 31.9% showed a tumor proportion score (TPS) ≥ 50% for PD-L1 (Table 1).

Table 2
Mutational profile of the NGS series from 131 tumors, as compared to our baseline mutational profile and the literature.

	NGS series*N* = 131	Database *N* = 660	*P*-Value	Literature[18]*
No mutation	25(19.1%)	181 (27.4%)		
At least 1 mutation	106 (80.9%)	479 (72.6%)	0.05	
	133	**611**		
Number of mutations				
KRAS	75(57.3%)	235 (35.6%)	<0.001	
				32.2%
TP53 (*N* = 80)	31(38.8%)	256 (38.8%)	NS	ND
EGFR	11(8.4%)	83 (12.6%)	0.08	11.3%
PIK3CA	7(5.3%)	14 (2.1%)	NS	ND
BRAF	2(1.5%)	21 (3.2%)	NS	7.0%
NRAS	1 (0.8%)	2 (<1.0%)	NS	0.4%
MET skipping ex14 (*N* = 51)	4(7.8%)	ND	ND	4.3%
MAP2K1(*N* = 51)	2(3.9%)	ND	ND	0.9%

**Ref:*The Cancer Genome Atlas Research Network, Disease analysis working group, Collisson E et al. Comprehensive molecular profiling of lung adenocarcinoma. *Nature* 2014; 511: 543–550. *NS: Not significant; ND: Not determined.*

Mutations detected by NGS

A total of 131 tumors were tested by NGS: two tumors in 52 patients (85.2%) and three tumors in nine patients (14.8%); Table 2. At least one mutation was found in 106 (80.9%) tumors. A single mutation was found in 78 tumors (59.5%), a double co-mutation in 27 tumors (20.6%) and triple co-mutations in one tumor (0.8%). *KRAS* was the most frequently mutated gene (75, 57.3%), with a rate significantly higher than expected compared to the frequencies identified in the Cancer Genome Atlas [18] ($p < 0.001$) (Table 2, Fig. 1, Supplementary figure 3); *EGFR* was mutated in 11 our of 131 tumors (8.4%), that was slightly lower than expected, without significant difference ($p = 0.08$). These results are most likely related to the high rate of smokers in our series.

TP53 gene was investigated only on the Illumina TST-15 panel and was mutated in 31 out of the 80 tested tumors (38.8%) and co-mutated in half of them (17/31, 54.8%), mainly with *KRAS* (14 cases). All five cases having a *PIK3CA* mutation were co-mutated, with KRAS for four of them and with EGFR for one (Supplementary figure 4). In one 83-year-old tyrosine kinase naïve non-smoking patient, three different *EGFR* mutations were found in two primary synchronous adenocarcinomas of the same lobe. One tumor harbored a co-mutation of *EGFR* (Leu858Arg) with *TP53* and the second tumor harbored another sensitizing *EGFR* mutation (exon 18 deletion) with the *de novo* T790M resistant mutation. A total of four patients (6.6%) showed a sensitizing *EGFR* mutation in one tumor and a *KRAS* mutation in the second tumor, underlying the importance of testing each of the multiple synchronous invasive tumors.

In table 3, the joint probability of mutations under the independence assumption is displayed for the 79 tumor pairs. Out of the 61 patients, 46 patients (75.4%) showed discordant molecular findings and 15 (24.6%) showed concordant molecular findings (Table 3). A total of 7 cases and 9 tumor pairs showed a probability < 1% of independence, corresponding to concordant low frequency scenarios.

Cases with concordant mutations

Among the 15 cases with concordant molecular findings, 3 had no mutation in either tumor, and 5 cases harbored the most frequent *KRAS* mutation G12C in both tumors. In these 8 cases with "non-informative" molecular results with regards to MPLC/IPM classification, the initial diagnosis (6 cases with MPLC, and 2 cases with IPM) remained unchanged. The joint probability of two tumors having no identified mutations was 13% by chance alone. The probability of identifying the most common *KRAS* mutation G12C in both tumors was 3% (Table 3).

In the 7 remaining cases with concordant mutations, there was a common low frequency mutation in both tumors, thus IPM was favored. The diagnosis was changed in four of these cases. In two cases, the diagnosis was amended from MPLC to IPM and restaged; in the third case the diagnosis was amended from IPM to metastatic recurrence of a contralateral adenocarcinoma resected 5 years earlier. In the fourth case, the diagnosis was amended from "not attributable" to IPM (Table 3).

Cases with discordant mutations

Among the 46 patients with discordant mutation profiles in both tumors, four cases were reclassified from IPM to MPLC. Also, four cases that were unclassified on histology were classified as MPLC (including cases with biopsies/ cytology).

In summary, the results were non-informative for 8 cases (13.1%), confirmed the initial diagnosis for 41 cases (67.2%) and allowed a diagnosis or changed the initial diagnosis for 12 patients (19.7%).

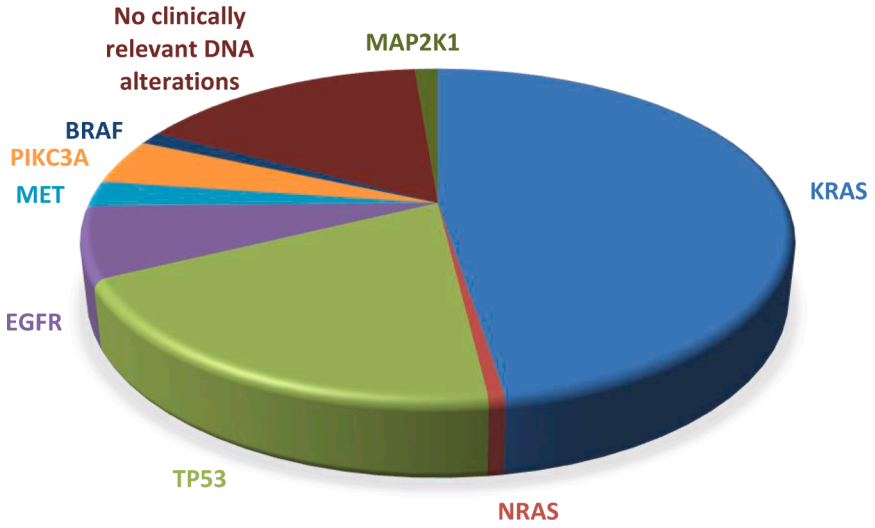

Fig. 1. Frequency of gene mutations in 131 tumors. *KRAS* was the most frequently mutated gene (75/131, 57.3%), at a rate higher than expected ($p < 0.001$); the *EGFR* mutation rate (11/131, 8.4%) was lower than expected in lung cancer ($p < 0.08$) . No mutation was detected in 25/131 tumors (19.1%).

Table 3
NGS results and impact on final staging.

Case #	Mutation	Joint-probability	Initial diagnosis ↓ Final Diagnosis
Discordant mutations/scenarios			
1	KRAS: c.34G > *T*; p.(Gly12Cys) TP53: c.730G > *T*; p.(Gly244Cys)	0.237412708	MPLC unchanged
2	KRAS: c.35G > *A*; p.(Gly12Asp), TP53:c292C > T; p.(Pro98Ser) KRAS: c.35G > *T*; p.(Gly12Val), TP53: c.818G > *T*; p.(Arg273Leu)	0.187020366	MPLC Unchanged
3	none detected KRAS: c.183A > C; p.(Gln61His)	0.138274186	MPLC Unchanged
4	none detected KRAS: c.34G > *T*; p.(G12C), TP53: c.955A > *T*; p.(Lys319*)	0.237412708	MPLC Unchanged
6	EGFR: c.2573T > *G*; p.(Leu858Arg) KRAS: c.38G > *A*; p.(Gly13Asp)	0.151082645	MPLC Unchanged
7a	none detected	0.15177463 (a and b)	MPLC Unchanged
7b	KRAS: c.35G > *A*; p.(Gly12Asp)	0.232593249 (a and c)	
7c	KRAS: c.34G > *T*; p.(Gly12Cys)	0.260592574 (b and c)	
8	KRAS: c.34_35delGGinsTC;p.(Gly12Ser) KRAS: c.34G > *T*; p.(Gly12Cys)	0.237412708	MPLC Unchanged
9	KRAS: c.37G > *T*; p.(Gly13Cys) none detected	0.138274186	MPLC Unchanged
10	KRAS: c.34G > *T*; p.(Gly12Cys), PIKC3A: c.1624G > *A*; p.(Glu542Lys) none detected	0.237412708	MPLC Unchanged
11	EGFR: c.2582T > *A*; p.(Leu861Gln), TP53: c.560–1Gly > Thr; Splice variant none detected	0.141139302	MPLC Unchanged
12	KRAS: c.34_35delGGinsTT;p.(Gly12Phe) KRAS: c.34G > *T*; p.(Gly12Cys)	0.237412708	MPLC Unchanged
13	TP53: c.473G > *T*; p.(Arg158Leu) none detected	0.138274186	MPLC Unchanged
14	KRAS: c.183A > C; p.(Gln61His) none detected	0.138274186	MPLC Unchanged
15	KRAS: c.35G > C; p.(Gly12Ala), PIKC3A: c.1624G > *A*; p.(Gly542Lys) KRAS: c.35G > *A*; p.(Gly12Asp)	0.165281496	MPLC Unchanged
16	KRAS: c.34G > *T*; p.(Gly12Cys) BRAF: c.1786G > C; p.(Gly596Arg)	0.237412708	MPLC Unchanged
17	KRAS: c.35G > *A*; p.(Gly12Asp) KRAS: c.37G > *T*; p.(Gly13Cys), PIKC3A: c.1633G > *A*; p.(Glu545Lys)	0.158129499	MPLC Unchanged
51	MAP2K1:c.171G > *T* (p.Lys57Asn) KRAS:c.35G > C (p.Gly12Ala); PIK3CA):c.1624G > *A* (p.Glu542Lys)	0.150579608	Not attributable ↓ MPLC
19	KRAS: c.34_35delGGinsTT;p.(Gly12Phe), TP53: c.376–1Gly > Cys; Splice variant KRAS: c.35G > C; p.(Gly12Ala)	0.147522854	MPLC Unchanged
20	TP53: c.469G > *T*; p.(Val157Phe) TP53: c.536A > *G*; p.(His179Arg)	0.141139302	MPLC Unchanged
21	none detected KRAS: c.34G > *T*; p.(Gly12Cys), TP53: c.383delC; p.(Pro128Lfs*42)	0.237412708	MPLC Unchanged
24	TP53: c.824G > *A*; p.(Cys275Tyr) KRAS: c.34G > *T*; p.(Gly12Cys)	0.237412708	MPLC Unchanged
26	KRAS: c.34G > *A*; p.(Gly12Ser), TP53: c.842A > *T*; p.(Asp281Val) KRAS: c.35G > *T*; p.(Gly12Val), TP53: c.742C > G; p.(Arg248Gly)	0.170384792	MPLC Unchanged
27	EGFR: c.2573T > *G*; p.(Leu858Arg), TP53: c.892G > *T*; p.(Glu298*) EGFR: c.2240_2257del18;p.(L747_P753delinsS) & c.2369C > T; p.(Thr790Met)	0.172777174	MPLC Unchanged
31	none detected NRAS: c.1824A > *T*; p.(Gln61Leu), TP53: c.730G > *T*;p.(Gly244Cys)	0.141139302	IPM ↓ MPLC
32	KRAS: c.34G > *T*; p.(Gly12Cys), TP53: c.818G > *T*; p.(Arg273Leu) KRAS: c.34G > *T*; p.(Gly12Cys)	0.031379999	IPM ↓ MPLC
34	KRAS: c.34G > *T*; p.(Gly12Cys) KRAS: c.35G > *T*; p.(Gly12Val)	0.275088929	MPLC Unchanged
36	KRAS:c.35G > C (p.Gly12Ala) none detected	0.144528152	MPLC Unchanged
37	none detected KRAS (p.Gly12Ala)	0.144528152	MPLC Unchanged
38	EGFR:c.2240_2257del18 (p.Leu747_Pro753delinsSer)		

(*continued on next page*)

Table 3 (*continued*)

	EGFR:c.2573T > *G* (p.Leu858Arg)	0.151082645	MPLC Unchanged
40	KRAS:c.183A > C (p.Gln61His) KRAS:c.34G > *T* (p.Gly12Cys)	0.237412708	MPLC Unchanged
41	MET:c.3028+3A > *T*; MET skipping exon 14 none detected	0.14801568	MPLC Unchanged
43c	KRAS:c.34G > *T* (p.Gly12Cys)	0.260592574 (a and b)	MPLC Unchanged
43b	KRAS:c.35G > *A* (p.Gly12Asp)	0.248150585 (b and c)	
43c	KRAS:c.35G > C (p.Gly12Ala)	0.161926295 (a and c)	
44	KRAS:c.34G >*T* (p.Gly12Cys) none detected	0.232593249	MPLC Unchanged
45	EGFR):c.2155G > *T* (p.Gly719Cys); EGFR:c.2303G > *T* (p.Ser768Ile) KRAS:c.35G > *T* (p.Gly12Val), PIK3CA:c.1133G > *T* (p.Cys378Phe), MET skipping exon 14	0.190225535	Not attributable ↓ MPLC
46	KRAS: c.34G > *T* (p.Gly12Cys); TP53:c.469G > *T* (V157F) KRAS: c.35G > *T* (p.Gly12Val)	0.280788922	Not attributable ↓ MPLC
48	KRAS:c.34G > *T* (p.Gly12Cys) KRAS:c.35G > *A* (p.Gly12Asp)	0.260592574	MPLC Unchanged
49	KRAS:c.34G > *T* (p.Gly12Cys) none detected	0.135467231	MPLC Unchanged
53	EGFR c.2156G > C KRAS:c.34G > *T* (p.Gly12Cys); TP53 c.383delC	0.242332028	MPLC Unchanged
54	BRAF: c.1790T > *A* KRAS: c.34G > *T*; p.(Gly12Cys)	0.237412708	MPLC Unchanged
55	KRAS: c.34G > *T*; p.(Gly12Cys) KRAS: c.34_35delGGinsTT;p.(Gly12Phe)	0.237412708	IPM ↓ MPLC
56	KRAS:c.35G > *T* (p.Gly12Val); MET exon 14 skipping EGFR: c.2573T > *G*; p.(Leu858Arg)	0.191274556	MPLC Unchanged
57a	None detected	0.138274186 (a and b)	MPLC Unchanged
57b	KRAS:c.35G > *A* (p.Gly12Asp)	0.160217614 (b and c)	
57c	KRAS: c.35G > *T*; p.(Gly12Val)	0.163537411 (a and c)	
58	None detected KRAS: c.34G > *T*; p.(Gly12Cys)	0.232593249	IPM ↓ MPLC
59a	KRAS: c.34G > *T*; p.(Gly12Cys)	0.248150585 (a and b)	MPLC Unchanged
59b	KRAS):c.35G > C (p.Gly12Ala)	0.275088929 (b and c)	
59c	KRAS: c.35G > *T*; p.(Gly12Val)	0.170934001 (a and c)	
60	None detected KRAS: c.35G > C (p.Gly12Ala); MAP2K1 c.605G > *T*	0.147522854	MPLC Unchanged
61	MET:c.3028G > *A* KRAS:c.34G > *T* (p.Gly12Cys)	0.254138567	Not attributable ↓ MPLC
Concordant mutations/scenarios**			
18	none detected none detected	0.135467231	MPLC NGS results not informative
30	none detected none detected	0.135467231	IPM NGS results not informative

(*continued on next page*)

Table 3 (*continued*)

42	none detected	0.135467231	IPM NGS results not informative
	none detected		
47	KRAS:c.34G > *T* (p.Gly12Cys)	0.030742988	MPLC NGS results not informative
	KRAS:c.34G > *T* (p.Gly12Cys)		
39	KRAS:c.35G > C (p.Gly12Ala)	0.000556135*	IPM unchanged
	KRAS:c.35G > C (p.Gly12Ala)		
35	TP53:c.442_457del16; p.(Asp148Pfs*17)	2.08E-05*	IPM Unchanged
	TP53:c.442_457del16; p.(Asp148Pfs*17)		
50	KRAS:c.34G > *T* (p.Gly12Cys); TP53:c.644G > *T* (p.S215I)	4.72E-06*	IPM Unchanged
	KRAS:c.34G > *T* (p.Gly12Cys); TP53:c.644G > *T* (p.S215I)		
52	EGFR: c.2573T > *G*; p.(Leu858Arg); PIK3CA c.3140 *A* > *G*	8.10E-08*	MPLC ↓
	EGFR: c.2573T > *G*; p.(Leu858Arg); PIK3CA c.3140 *A* > *G*		IPM
28	TP53: c.818G > *T*; p.(Arg273Leu)	2.08E-05*	MPLC ↓
	TP53: c.818G > *T*; p.(Arg273Leu)		IPM
29	KRAS: c.34G > *T*;p.(Gly12Cys), TP53: c.1006G > *T*; p.(Glu336*)	4.72E-06*	Not attributable ↓
	KRAS: c.34G > *T*; p.(Gly12Cys), TP53: c.1006G > *T*; p.(Glu336*)		IPM
33a	TP53: c.818G > *A*; p.(Arg273His)	2.08E-05* (a and b)	IPM ↓
33b	TP53: c.818G > *A*; p.(Arg273His)	2.08E-05* (b and c)	M1
33c	TP53: c.818G > *A*; p.(Arg273His)	2.08E-05* (a and c)	
5a	TP53: c.412G > C; p.(Ala138Pro)	0.237412708 (a and b)	MPLC NGS results not informative
5b	KRAS: c.34G > *T*; p.(Gly12Cys)	0.237412708 (a and c)	
5c	KRAS: c.34G > *T*; p.(Gly12Cys)	0.030742988 (b and c)	
22a	KRAS: c.34G > *T*; p.(Gly12Cys)	0.030742988 (a and b) 0.275088929 (b and c) 0.275088929 (a and c)	MPLC NGS results not informative
22b	KRAS: c.34G>*T*; p.(Gly12Cys)	0.275088929 (b and c)	
22c	KRAS: c.35G > *T*; p.(G12V)	0.275088929 (a and c)	
23a	KRAS: c.34G > *T*; p.(Gly12Cys)	0.030742988 (a and b))	MPLC NGS results not informative
23b	KRAS: c.34G > *T*; p.(Gly12Cys)	0.242332028 (b and c)	
23 c	TP53: c.657delC; p.Tyr220fs*27	0.242332028 (a and c)	
25a	none detected	0.232593249 (a and b)	MPLC NGS results not informative
25b	KRAS: c.34G > *T*; p.(Gly12Cys)	0.232593249 (b and c)	
25c	KRAS: c.34G > *T*; p.(Gly12Cys)	0.030742988 (a and c)	

The NGS results of the 79 pairs (131 tumors) from the 61 patients are detailed, including three pairs for each of the cases having three tumors tested. Joint probability is the probability of having these results by chance alone. Cases where the final diagnosis was changed arehhighlighted cases in gray.*P-Value <0.01. **at least two concordant mutations/scenarios.

Survival analysis

We investigated whether classification into IPM or MPLC categories affected the overall survival in a univariate analysis. Among the eight cases diagnosed as IPM with available follow-up, three cases died (4, 17 and 21 months) and two cases presented with distant metastasis (40 and 47 months). There was no statistical difference in survival outcomes between the two groups ($p = 0.4$, Fig. 2).

Discussion

Distinguishing between MPLC and IPM is critical in lung cancer as pathological stage, prognosis and treatment offered to patients is radically different. While the 8th edition of the TNM has attempted to

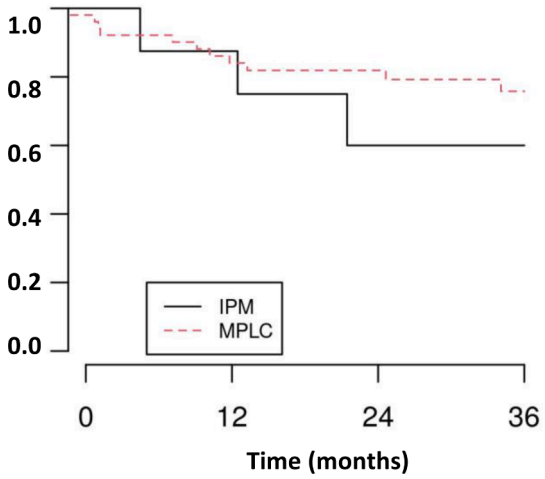

Fig. 2. Overall survival of patients. Classification into IPM or MPLC categories did not affect the overall survival in a univariate analysis. There was no statistically significant difference in survival outcomes between the two groups ($p = 0.4$).

standardize terminology for classification of multiple tumor sites, there remain limitations and risks of misclassification (Supplementary Figure 5 and 6). NGS platforms offer a promising mechanism to resolve this dilemma, but these have been described in small series and applied retrospectively [19–23]. We demonstrate that reflex NGS testing of multiple tumor foci very frequently provides added value to pathologists in the classification of stage of IPM and MPLC.

Over-reliance on molecular characterization may be misleading. Both tumors may be negative for the set of genes analyzed by NGS, especially in a focussed panel, and the test may be non-contributory; the tumours may evolve and acquire new molecular changes leading to (false) discordant molecular profile with different mutational profile between the primary tumor and metastases, [24] or intratumoral heterogeneity may lead to different results (sampling bias) [25]. However, focussed NGS panels investigate mainly mutations in driver genes [12, 19-23]' [26–30]. Driver mutations are usually early events, concordant between the primary tumor and metastases, [31] whereas the risk of molecular heterogeneity is higher for passenger mutations.

To contextualize the NGS results in the two (and occasionally three) tumors we used a probabilistic model where we computed for each pair, the probability of observing such a pattern under the hypothesis of being multiple primary lung cancer. Importantly, we included in the model the dependencies between driver mutations. For example, where two mutations may be mutually exclusive, we included this negative interdependency in the model. This allowed us to determine the joint probability of these mutations identified in the two tumors under the hypothesis that they occur by chance alone for each tumor pair.

The NGS results were the most useful in cases of concordant mutations, where the mutation frequency was low. For example, *TP53* analysis for assessing clonality was particularly useful. This large gene harbors numerous possible mutations, each of them having low frequency and the risk to share one specific *TP53* mutation coincidentally is a highly unlikely event to encounter by chance alone. In these cases, despite being classified as MPLC, these were reclassified to IPM, resulting in important changes in treatment and prognosis. In cases of concordant mutations which occurred with a high frequency, the NGS was less useful. For example, the common *KRAS* G12C mutation occurs in one third of lung cancers. [32] We found the probability of two tumors, having this high frequency mutation by chance alone, is not insignificant (joint probability 3%) and could not rule out the possibility of MPLC. In our study, five cases initially diagnosed as MPLC shared the most frequent *KRAS* G12C mutation in at least two tumors. Similarly, the joint occurrence of the high frequency scenario of having no mutation identified in either tumor (joint probability 13.5%), or one tumor with a high frequency mutation and the other with no mutation (joint probability varied between 13.5 and 23.7%) did not change the possibility that this may occur by chance alone.

Our case series identified a predominance of women with multiple lung adenocarcinomas, and a predominance of smokers or ex-smokers. In particular, the occurrence of *KRAS* mutations in more than half of the patients with two or more tumors was more frequent than both our local incidence of *KRAS* mutation in solitary lung cancers, and published incidences. Unlike other case series of Asian patients with multiple primary lung cancers, we found a trend for a low incidence of *EGFR* mutations, but it was not statistically significant. [20]

In our study, we used NGS gene panels from Illumina focusing on either 15 or 52 genes. Larger panels or different gene panels may enhance the effectiveness of calling lineages but are still non-informative in 14% of lung cancers. [22] Other types of molecular analyses such as deep sequencing with analysis of overlapping mutations [33], and genomic breakpoint junctions from structural rearrangements [22] are promising methodologies for discrimination of MPLC and IPM, however they are more labor intensive than the commonly used NGS panels. Also, low coverage whole genome sequencing or SNP arrays may be used. However, this technology is not yet widely available in the diagnostic setting. As such, the combination of routine panel NGS and probability assessment with the CHA provides an evaluation of important broadly available tools for laboratories which do not have access to whole genome analysis.

One limitation to our study was that the 52-gene panel did not probe for the *TP53* gene mutations which were helpful in differentiating IPM from MPLC in a number of cases in our series. This finding would support the inclusion of *TP53* in NGS panels aimed at use in lung cancer patients.

Our series identified tumors mostly obtained from surgically resected patients with MPLC (52/61, 85.2%). This high rate may reflect selection bias towards patients with multiple primaries in our center. With large areas of tumors tested available from surgical specimens, it is unlikely than discordant results (mutation in one tumor and not the other) is a result of sampling bias.

The overall survival analysis showed no statistically significant difference between IPM and MPLC groups. These findings might be due to the relatively small sample size of our IPM series thus the statistical power to detect a difference was low. Larger series are needed to validate the potential clinical usefulness of these categorizations.

Conclusion

In summary, our study shows that the NGS testing is a useful tool for differential diagnosis of multiple lung adenocarcinomas and should be integrated with histological parameters for refining the diagnosis between IPM and MPLC. Using a statistical score based on NGS data that estimates the probability of two mutations occurring in more than one tumor site in the same patient occurring by chance versus being indicative of a common clonal origin may significantly improve accuracy of diagnosis, staging, and therefore treatment planning and prognostication.

Clinical practice points

- Distinguishing between MPLC and IPM is critical in lung cancer as pathological stage, treatment and prognosis may be radically different.
- NGS platforms offer a promising mechanism to distinguish between MPLC and IPM
- Focussed NGS panels investigate mainly mutations in driver genes
- Using a probabilistic model allowed us to determine the joint probability of the mutations identified in the two tumors under the hypothesis that they occur by chance alone for each tumor pair.

- The NGS results were the most useful in cases of concordant mutations, where the mutation frequency was low, while they were less useful in cases of concordant mutations which occurred with a high frequency.
- Our case series identified a predominance of women with multiple lung adenocarcinomas, and a predominance of smokers or ex-smokers with high incidence of *KRAS*.

Data statement

The datasets used and/or analyzed during the current study are available from the corresponding author on reasonable request.

Disclosure of funding received

- Grant from the Division of Pathology, MUHC and the MGH Foundation

Author contributions

SCB and NE take responsibility for the content of the manuscript, including the data and analysis. SCB, NE, AB, POF, PB, JS contributed to the study design. SCB, HW, AG, POF, AB, LVK, GC, AS, RF, JBR, MI contributed to data collection. PB, SCB performed statistical analysis and interpretation. NE, SCB, JS, PB, MI drafted and revised the manuscript. All authors contributed to critical revision of the manuscript and approved its final version.

Declaration of Competing Interest

Drs. Ezer, Wang, Gomez, Baig, Chong, Issac, Fraser, Spatz, Riviere, Broët and Camilleri-Broët have nothing to disclose. Dr. van Kempen reports grants, personal fees and non-financial support from Roche, personal fees from AstraZeneca, personal fees from Novartis, grants and non-financial support from Invitae, non-financial support from Biocartis, personal fees from Merck, personal fees from Janssen-Cilag, grants and personal fees from Bayer, personal fees from BMS, personal fees and non-financial support from nanoString, personal fees from Pfizer, outside the submitted work; Dr. Fiset reports personal fees from Amgen, personal fees from EMD Serono, personal fees from Bristol Myers Squibb, personal fees from AstraZeneca, personal fees from Merck Canada, personal fees from Pfizer Canada, personal fees from Roche Canada, outside the submitted work; .Dr. Spicer reports grants and personal fees from Astra Zeneca, personal fees from BMS, grants and personal fees from Merck, grants from Roche, personal fees from Protalix, grants from CLS therapeutics, personal fees from Transhit Bio, outside the submitted work

Acknowledgement

We would like to thank the Division of Pathology, MUHC and the MGH Foundation for providing grants to conduct this research.

Supplementary materials

Supplementary material associated with this article can be found, in the online version, at doi:10.1016/j.ctarc.2021.100484.

References

[1] F.C. Detterbeck, D.J. Boffa, A.W. Kim, et al., The eighth edition lung cancer stage classification, Chest 151 (1) (2017) 193–203, https://doi.org/10.1016/j.chest.2016.10.010. Jan.

[2] F.C. Detterbeck, A.G. Nicholson, W.A. Franklin, et al., IASLC staging and prognostic factors committee; advisory boards; multiple pulmonary sites workgroup; participating institutions. The IASLC lung cancer staging project: summary of proposals for revisions of the classification of lung cancers with multiple pulmonary sites of involvement in the forthcoming eighth edition of the TNM classification, J. Thorac. Oncol. 11 (5) (2016) 639–650, https://doi.org/10.1016/j.jtho.2016.01.024. May.

[3] F.C. Detterbeck, V. Bolejack, D.A. Arenberg, et al., IASLC staging and prognostic factors committee; advisory boards; multiple pulmonary sites workgroup; participating institutions. The IASLC lung cancer staging project: background data and proposals for the classification of lung cancer with separate tumor nodules in the forthcoming eighth edition of the TNM classification for lung cancer, J. Thorac. Oncol. 11 (5) (2016) 681–692, https://doi.org/10.1016/j.jtho.2015.12.114. May.

[4] F.C. Detterbeck, W.A. Franklin, A.G. Nicholson, et al., IASLC staging and prognostic factors committee; advisory boards; multiple pulmonary sites workgroup. the iaslc lung cancer staging project: background data and proposed criteria to distinguish separate primary lung cancers from metastatic Foci in patients with two lung tumors in the forthcoming eighth edition of the TNM classification for lung cancer, J. Thorac. Oncol. 11 (5) (2016) 651–665, https://doi.org/10.1016/j.jtho.2016.01.025. May.

[5] F.C. Detterbeck, E.M. Marom, D.A. Arenberg, et al., IASLC staging and prognostic factors committee; advisory boards; multiple pulmonary sites workgroup. the iaslc lung cancer staging project: background data and proposals for the application of tnm staging rules to lung cancer presenting as multiple nodules with ground glass or lepidic features or a pneumonic type of involvement in the forthcoming eighth edition of the TNM classification, J. Thorac. Oncol. 11 (5) (2016) 666–680, https://doi.org/10.1016/j.jtho.2015.12.113. May.

[6] N. Martini, M.R. Melamed, Multiple primary lung cancers, J. Thorac. Cardiovasc. Surg. 70 (4) (1975) 606–612.

[7] N. Girard, C. Deshpande, C. Lau, et al., Comprehensive histologic assessment helps to differentiate multiple lung primary nonsmall cell carcinomas from metastases, Am. J. Surg. Pathol. 33 (2009) 1752–1764, https://doi.org/10.1097/PAS.0b013e3181b8cf03.

[8] A.G. Nicholson, K. Torkko, P. Viola, et al., Interobserver variation among pathologists and refinement of criteria in distinguishing separate primary tumors from intrapulmonary metastases in lung, J. Thorac. Oncol. 13 (2) (2018) 205–217, https://doi.org/10.1016/j.jtho.2017.10.019.

[9] S.D. Moffatt-Bruce, P. Ross, M.E. Leon, et al., Comparative mutational profiling in the assessment of lung lesions: should it be the standard of care? Ann. Thorac. Surg. 90 (2) (2010) 388–396, https://doi.org/10.1016/j.athoracsur.2010.03.059. Aug;.

[10] Travis W.D., Noguchi M., Yatabe Y., et al. Adenocarcinoma. In: Travis WD, Brambilla E, Burke AP, Marx A, Nicholson AG, Eds.. WHO Classification of Tumours of the Lung, Pleura, Thymus and Heart. 4 ed. Lyon, France: International Agency for Research on Cancer; 2015. p. 26–50.

[11] H. Cheng, B.F. Lei, P.J. Peng, et al., Histologic lung cancer subtype differentiates synchronous multiple primary lung adenocarcinomas from intrapulmonary metastases, J. Surg. Res. 211 (2017) 215–222, https://doi.org/10.1016/j.jss.2016.11.050. May 1.

[12] A. Mansuet-Lupo, M. Barritault, M. Alifano, et al., Proposal for a combined histomolecular algorithm to distinguish multiple primary adenocarcinomas from intrapulmonary metastasis in patients with multiple lung tumors, J. Thorac. Oncol. (5) (2019) 844–856, https://doi.org/10.1016/j.jtho.2019.01.017. May; 14.

[13] W.D. Travis, E. Brambilla, A.G. Nicholson, et al., The 2015 world health organization classification of lung tumors: impact of genetic, clinical and radiologic advances since the 2004 classification, J. Thorac. Oncol. 10 (9) (2015) 1243–1260, https://doi.org/10.1097/JTO.0000000000000630.

[14] W.D. Travis, I.A.S.L.C. Staging Committee, Reporting lung cancer pathology specimens, in: Impact of the Anticipated 7th Edition TNM Classification Based On Recommendations of the IASLC Staging Committee, 54, Histopathology, 2009, pp. 3–11, https://doi.org/10.1111/j.1365-2559.2008.03179.x. Jan.

[15] M.B. Amin, S.B. Edge, F.L. Greene, et al., AJCC Cancer Staging Manual, eds, Springer, New York, NY, 2017, 8th ed.

[16] M.M. Li, M. Datto, E.J. Duncavage, et al., Standards and Guidelines for the Interpretation and Reporting of Sequence Variants in Cancer: A Joint Consensus Recommendation of the Association for Molecular Pathology, 19, American Society of Clinical Oncology, and College of American Pathologists. J Mol Diagn, 2017, pp. 4–23, https://doi.org/10.1016/j.jmoldx.2016.10.002.

[17] M.H. Bailey, W.U. Meyerson, L.J. Dursi, et al., Retrospective evaluation of whole exome and genome mutation calls in 746 cancer samples, Nat. Commun. 11 (2020) 4748, https://doi.org/10.1038/s41467-020-18151-y.

[18] Disease analysis working group The Cancer Genome Atlas Research Network, E. Collisson, et al., Comprehensive molecular profiling of lung adenocarcinoma, Nature 511 (2014) 543–550, https://doi.org/10.1038/nature13385.

[19] R. Zheng, Q. Shen, S. Mardekian, et al., Molecular profiling of key driver genes improves staging accuracy in multifocal non-small cell lung cancer, J. Thorac. Cardiovasc. Surg. 160 (2) (2020) e71–e79, https://doi.org/10.1016/j.jtcvs.2019.11.126.

[20] X. Chen, J. Lu, Y. Wu, et al., Genetic features and application value of next generation sequencing in the diagnosis of synchronous multifocal lung adenocarcinoma, Oncol. Lett. 20 (3) (2020) 2829–2839, https://doi.org/10.3892/ol.2020.11843.

[21] E. Donfrancesco, V. Yvorel, F. Casteillo, et al., Histopathological and molecular study for synchronous lung adenocarcinoma staging, Virchows Arch. 476 (6) (2020) 835–842, https://doi.org/10.1007/s00428-019-02736-0.

[22] S.J. Murphy, F.R. Harris, F. Kosari, et al., Using Genomics to differentiate multiple primaries from metastatic lung cancer, J. Thorac. Oncol. 14 (9) (2019) 1567–1582, https://doi.org/10.1016/j.jtho.2019.05.008.

[23] D. Berry, M. Mahadevan, M.R. Wick, Detection of synchronous primary lung adenocarcinomas with genomic sequencing, Ann. DiagnPathol. 34 (2018) 42–44, https://doi.org/10.1016/j.anndiagpath.2018.01.007.

[24] H.S. Han, D.W. Eom, J.H. Kim, et al., EGFR mutation status in primary lung adenocarcinomas and corresponding metastatic lesions: discordance in pleural metastases, Clin. Lung Cancer (6) (2011) 380–386, https://doi.org/10.1016/j.cllc.2011.02.006. Nov; 12.
[25] M. Jamal-Hanjani, A. Hackshaw, Y. Ngai, et al., Tracking genomic cancer evolution for precision medicine: the lung TRACERx study, PLoS Biol. 12 (7) (2014), e1001906, https://doi.org/10.1371/journal.pbio.1001906. Jul 8.
[26] C.A. Pagan, C.A. Shu, J.P. Crapanzano, et al., Synchronous pulmonary adenocarcinomas, Am. J. Clin. Pathol. 154 (1) (2020) 57–69, https://doi.org/10.1093/ajcp/aqaa023. Jun8.
[27] J.C. Chang, D. Alex, M. Bott, et al., Comprehensive next-generation sequencing unambiguously distinguishes separate primary lung carcinomas from intrapulmonary metastases: comparison with standard histopathologic approach, Clin. Cancer Res. 25 (23) (2019) 7113–7125, https://doi.org/10.1158/1078-0432.CCR-19-1700. Dec.
[28] P. Roepman, A. Ten Heuvel, K.C. Scheidel, et al., Added value of 50-gene panel sequencing to distinguish multiple primary lung cancers from pulmonary metastases: a systematic investigation, J. Mol. Diagn. 20 (4) (2018) 436–445, https://doi.org/10.1016/j.jmoldx.2018.02.007. Jul.
[29] J. Saab, H. Zia, S. Mathew, et al., Utility of genomic analysis in differentiating synchronous and metachronous lung adenocarcinomas from primary adenocarcinomas with intrapulmonary metastasis, Transl. Oncol. 10 (3) (2017) 442–449, https://doi.org/10.1016/j.tranon.2017.02.009. Jun.
[30] F.K. Bruehl, E.E. Doxtader, Y.W. Cheng, et al., Does histological assessment accurately distinguish separate primary lung adenocarcinomas from intrapulmonary metastases? A study of paired resected lung nodules in 32 patients using a routine next-generation sequencing panel for driver mutations, J. Clin. Pathol. (2021), https://doi.org/10.1136/jclinpath-2021-207421. Marjclinpath-2021-207421.
[31] S. Vignot, G.M. Frampton, J.C. Soria, et al., Next-generation sequencing reveals high concordance of recurrent somatic alterations between primary tumor and metastases from patients with non-small-cell lung cancer, J. Clin. Oncol. 31 (17) (2013) 2167–2172, https://doi.org/10.1200/JCO.2012.47.7737. Jun 10.
[32] https://www.mycancergenome.org/content/alteration/kras-g12c/.
[33] J. Liu, G. Mao, Y. Li, et al., Targeted deep sequencing helps distinguish independent primary tumors from intrapulmonary metastasis for lung cancer diagnosis, J. Cancer Res. Clin. Oncol. 146 (9) (2020) 2359–2367, https://doi.org/10.1007/s00432-020-03227-5. Sep.